A New Framework for Dealing with Input Constraints on Parallel Interconnection of Buck Converters

Jérémie Kreiss, Jean-François Trégouët, Romain Delpoux, Jean-Yves Gauthier, Xuefang Lin-Shi

A New Framework for Dealing with Input Constraints on Parallel Interconnection of Buck Converters

Jérémie Kreiss[1], Jean-François Trégouët[1], Romain Delpoux[1], Jean-Yves Gauthier[1] and Xuefang Lin-Shi[1]

***Abstract*— This paper tackles the current sharing problem for interconnected power converters. Specifically, it considers a single load, fed by parallel buck converters via a common DC bus. In such a case, it has been recently shown that dynamics related to current distribution can be controlled without impacting voltage regulation. Such a decoupling is performed without resorting to frequency separation argument, which inevitably lowers achievable performance. This decoupling can be destroyed by input constraints, though. In this context, this paper shows that a mere unilateral coupling can still be achieved: Using a novel control structure, foremost control goal of voltage regulation can be made independent of current distribution control. Controller design example exploiting the control scheme is provided together with numerical simulations.**

I. Introduction

Nowadays, connecting several power converters in parallel to a single load becomes more and more common. Indeed, in many applications such as simplified Microgrids (see [1] for example) or Low-voltage/High-current power supplies, this kind of parallel interconnection of converters is used. Despite a larger number of electrical components, this interconnection benefits from several advantages such as increased reliability, ease of maintenance and repair, improved thermal management, reduced output ripple by interleaving phase of Pulse Width Modulation (PWM), etc. Each of them being a consequence of the possibility to freely distribute the load current on each converter.

Several solutions for controlling such a system have been proposed in the literature (see e.g. [2], [3], [4]). The main challenge is to separately regulate output voltage, which is the main control objective, as well as current distribution, the secondary control objective. Those two dynamics are coupled, though. To cope with this difficulty, most of existing solutions resort to control design procedure relying on several SISO transfer functions shaping. However, deriving conditions for closed-loop stability in this framework seems rather involved, so that frequency separation is often ultimately used as the key argument, which inevitably lowers achievable performance by imposing a slow current distribution dynamics, see e.g. [5], [6], [7], [1]. Furthermore input constraints are seldom taken into account. It is a point of main interest though, knowing that duty cycles must belong to $[0,1]$.

In stark contrast with this approach, new solution has been recently proposed in [8], [9], resorting to both state and input change of coordinates rather than frequency separation to completely separate voltage and current distribution dynamics, hence offering tractability without sacrificing performance. Such an approach is applicable for arbitrary number of DC/DC buck converters, possibly having distinct characteristics. As shown in [9], roots of this solution can be tracked back to early work on geometric control theory (see [10], [11], [12]).

Building on [8], [9], a step further is made in this paper by explicitly take input constraints into account. It is shown that the naive solution consisting in saturating duty cycles restores a bilateral coupling between voltage and current distribution dynamics. Yet, deeper investigations reveal that voltage regulation can still be made independent from current distribution dynamics. To clarify this point, one should distinguish between two different kind of saturations:

(i) the one occurring when input component related to output voltage dynamics (roughly the sum of duty cycles of all converters) reaches its limit,
(ii) the one happening when input limitations merely imposes reconfiguration without modifying input component mentioned above.

The intuition is that the latter is somehow less "concerning" than the former, in the sense that experiencing (ii) without (i) leaves input corresponding to output voltage, and in turn voltage trajectory itself, unaffected by input limits if properly treated, i.e. simple input reconfiguration is required. Our main contribution in this paper is to provide a control scheme performing post-treatment of the desired input vector (the one computed in an unsaturated context) in such a way that input direction related to main control objectives is preserved from input limitations, as much as possible. Simulation results show that such a strategy allows to use full capacity of the system subjected to input limitations.

Notation: The symbol $\mathbf{I}_m$ stands for the identity matrix of dimensions $m \times m$. The null matrix of size $m \times n$ is denoted by $\mathbf{0}_{m\times n}$. The vector (column matrix) of size m for which every entry is 1 (0) is denoted by $\mathbf{1}_m$ ($\mathbf{0}_m$). The notation x_k refers to the k-th element of the vector x, with 1 being the index of the first element. The operator "diag" builds diagonal matrix from entries of the input vector argument. Let $y,z \in \mathbb{R}^p$ two vectors of size p. Relation $y \leq z$ (resp. $y < z$) must be read as the following p inequalities $y_k \leq z_k$ (resp. $y_k < z_k$) for all $k \in \{1,\dots,p\}$. The inverse of any vector $y \in \mathbb{R}^p$ for which $y_k \neq 0$, ($k \in \{1,\dots,p\}$) corresponds to component-wise inversion, i.e.

$$y^{-1} := \mathrm{diag}\,\{y\}^{-1}\,\mathbf{1}_p = [1/y_1,\dots,1/y_p]^\intercal.$$

[1]Every author is with Laboratoire Ampère, INSA Lyon, Université de Lyon, 20, Avenue Albert Einstein, 69100 Villeurbanne, France firstname.lastname@insa-lyon.fr

II. Problem statement

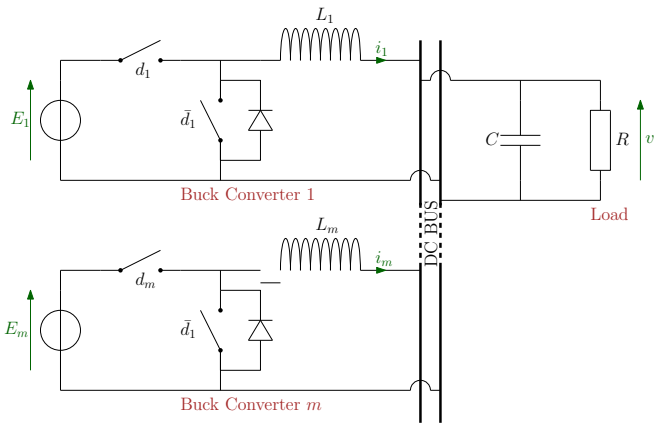

Fig. 1. Electrical schematic

We consider the electrical circuit depicted by Fig. 1 where m DC/DC buck converters are connected in a parallel way to a resistive load R through a single capacitor C. Converters are controlled via PWM signals where d_k refers to duty-cycle of the k-th converter. Index k belongs to the set $\mathscr{K} := \{1,\dots,m\}$ and duty cycles are constrained by the following relationship

$$d \in [0,1]^m. \tag{1}$$

Voltage of DC bus is denoted by v whereas current in k-th inductor L_k is referred to as i_k. Gather all those state variables to obtain the following state vector: $\mathbb{R}^n \ni x := \left[i^\intercal v\right]^\intercal$ where $i = \left[i_1,\dots,i_m\right]^\intercal$ and $n := m+1$. Magnitude of voltage sources E_k are supposed to be known and constant.

Throughout this paper, we assume that (i) switching frequency f_s is sufficiently large for the dynamics to be approximated by an average continuous time model, (ii) converters remain in continuous conduction mode and (iii) electrical components and switches are ideals, i.e. parasitic elements (resistances, losses) can be neglected.

From Kirchoff's laws, one can easily verify (see [8]) that dynamics reads

$$\begin{bmatrix} \operatorname{diag}\{L\} & \mathbf{0} \\ \mathbf{0} & C \end{bmatrix} \dot{x} = \begin{bmatrix} \mathbf{0} & -\mathbf{1}_m \\ \mathbf{1}_m^\intercal & -1/R \end{bmatrix} x + \begin{bmatrix} \operatorname{diag}\{E\} \\ \mathbf{0}_m^\intercal \end{bmatrix} d \tag{2}$$

Main control objective of system (2) is to regulate output voltage v.

However, controlling (2) with the only goal of regulating the output voltage does not address all degrees of freedom. For this reason, a second control objective is considered: Distribute the total current on each converters according to a given reference. This reference might come from the minimization of a cost function. Note that this formulation encompasses the objective of minimization power losses, as considered in [13] where the power losses model is different from the control model and takes internal resistors into account. Since goal of power converters is to regulate output voltage, priority is given to this objective in the case where the two control goals are competing. In light of this observation, problem tackles in the paper is now defined.

Problem 1: For system (2) with duty cycles constrained as in (1), define a state-feedback addressing the two following control objectives:

(a) regulate the output voltage v to v_r;
(b) regulate the current repartition to a reference value δ_r

Objective (a) always has priority over objective (b).

III. The unconstrained context

Geometric control theory provides important tools for dealing with distinct control objectives. Indeed, in [11], [14] we find a useful decomposition based on the existence of invariant subspaces. In fact, this decomposition relies on:

(i) change the coordinates isolating smallest part of both input and state variables that act on objective (a) from the remaining variables which will be used for objective (b);
(ii) performing a controllers in two parts, the first one for objective (a) and the second one for objective (b).

Based on this approach, [8] proposes a control framework which can be used for solving Problem 1 in the unconstrained context. The interested reader is referred to [9] for more details about the origin of the change of coordinates introduced in this section.

A. A useful decomposition

Select new state variables $(\delta,\sigma,v) \in \mathbb{R}^{m-1}\times\mathbb{R}\times\mathbb{R}$ via

$$\begin{bmatrix} \delta \\ \sigma \\ v \end{bmatrix} = T^{-1}x \text{ with } T^{-1} := \begin{bmatrix} \Gamma_m^\intercal & \mathbf{0}_{m-1} \\ \mathbf{1}_m^\intercal & 0 \\ \mathbf{0}_m^\intercal & 1 \end{bmatrix} \in \mathbb{R}^{n\times n} \tag{3}$$

where $\Gamma_m \in \mathbb{R}^{m\times(m-1)}$ is defined as follows

$$\Gamma_m := \begin{bmatrix} I_{m-1} & \mathbf{0}_{m-1} \end{bmatrix}^\intercal - \begin{bmatrix} \mathbf{0}_{m-1} & I_{m-1} \end{bmatrix}^\intercal. \tag{4}$$

Note that T is indeed invertible and it can be easily verified that this matrix reads

$$T = \begin{bmatrix} \Gamma_m(\Gamma_m^\intercal\Gamma_m)^{-1} & \frac{1}{m}\mathbf{1}_m & \mathbf{0}_m \\ \mathbf{0}_{m-1}^\intercal & 0 & 1 \end{bmatrix}. \tag{5}$$

Regarding the input, perform following change of coordinates

$$d = \begin{bmatrix} G_{\lambda\to d} & G_{\mu\to d} \end{bmatrix} \begin{bmatrix} \lambda \\ \mu \end{bmatrix} \tag{6}$$

with

$$\mathbb{R}^{m\times(m-1)} \ni G_{\lambda\to d} := \operatorname{diag}\{E\}^{-1}\operatorname{diag}\{L\}\Gamma_m(\Gamma_m^\intercal\Gamma_m)^{-1}E_\delta L_\delta^{-1}$$

and

$$\mathbb{R}^{m\times 1} \ni G_{\mu\to d} := \operatorname{diag}\{E\}^{-1}\operatorname{diag}\{L\}\frac{1}{m}\mathbf{1}_m\frac{E_{\text{eq}}}{L_{\text{eq}}}$$

which decomposes d into $\lambda \in \mathbb{R}^{m-1}$ and $\mu \in \mathbb{R}$. Here, the following notations have been used:

$$E_\delta := \operatorname{diag}\{\Delta^* E\}, \qquad L_\delta := \operatorname{diag}\left\{\Delta^*(L^{-1})\right\}^{-1},$$
$$\mathbb{R}^{+*} \ni 1/L_{\text{eq}} := \sum_k 1/L_k, \qquad \mathbb{R}^{+*} \ni E_{\text{eq}} := \min_k E_k,$$

and operator Δ reads $\mathbb{R}^p \ni y \mapsto \Delta y := \Gamma_p^{\mathsf{T}} y$, whereas [1] Δ^* is such that:

$$\mathbb{R}^p \ni y \mapsto (\Delta^* y)_k := \begin{cases} (\Delta y)_k, & (y_k \neq y_{k+1}) \\ 1, & (\text{otherwise.}) \end{cases}$$

Resulting dynamics of the open-loop in the new coordinates can be decomposed into a cascaded form where upper subsystem Σ_v, defined by

$$\Sigma_v : \frac{\mathrm{d}}{\mathrm{d}t}\begin{bmatrix}\sigma \\ v\end{bmatrix} = \begin{bmatrix} 0 & -\frac{1}{L_{\text{eq}}} \\ \frac{1}{C} & -\frac{1}{RC}\end{bmatrix}\begin{bmatrix}\sigma \\ v\end{bmatrix} + \begin{bmatrix}E_{\text{eq}}/L_{\text{eq}} \\ 0\end{bmatrix}\mu, \qquad (7)$$

feeds a lower one, denoted by Σ_δ and governs by

$$\Sigma_\delta : \ \dot{\delta} = -\Delta(L^{-1})v + E_\delta L_\delta^{-1}\lambda. \qquad (8)$$

Remark (Physical interpretation and ordered objectives).
It is worth mentioning that the new state variable σ corresponds to the total current and that the new sub state vector δ admits a physical interpretation as it holds $\delta = [(i_1 - i_2), (i_2 - i_3), \ldots, (i_{m-1} - i_m)]^{\mathsf{T}}$ so that this vector reflects the current distribution. ⌟

B. Control design with respect to the decomposition

Σ_v and Σ_δ are Linear systems. The purpose being to illustrate the paper results, we assume here that the load R is known such as in [9] and we consider the following state-feedback controllers

$$\mathscr{C}_v : \qquad \mu = K_v\left(\begin{bmatrix}\sigma \\ v\end{bmatrix} - \begin{bmatrix}v_r/R \\ v_r\end{bmatrix}\right) + \frac{v_r}{E_{\text{eq}}} \qquad (9)$$

$$\mathscr{C}_\delta : \qquad \lambda = K_\delta(\delta - \delta_r) + L_\delta E_\delta^{-1}\Delta(L^{-1})v. \qquad (10)$$

where $K_v \in \mathbb{R}^{1\times 2}$ and $K_\delta \in \mathbb{R}^{(m-1)\times(m-1)}$ are chosen to make the closed-loops Hurwitz. Thus equilibrium verify $v = v_r$ and $\delta = \delta_r \in \mathbb{R}^{m-1}$ and solve Problem 1 in the unconstrained case.

Note that we can apply any methodology from the literature to control it, including when R is unknown. Development of this paper can be straightforwardly derived to any other control structure.

IV. A First Naive Solution

In previous section, design of a controller that solve Problem 1 in the unconstrained case has been proposed. This controller might deliver infeasible duty-cycles, though. This happens when $d = G_{\lambda\to d}\lambda + G_{\mu\to d}\mu$ does not belong to $[0,1]^m$. A naive solution is to simply saturate the duty-cycles d as a post-treatment of the signal delivered by controller constructed in Sec. III. This means that entries of the "desired" duty-cycle vector $G_{\lambda\to d}\lambda_d + G_{\mu\to d}\mu_d$ are individually saturated to be in $[0,1]$. This solution is depicted on Fig. 2. Vis-a-vis previous section, only a saturation block is inserted after input change of coordinates matrix G and before system model.

In such a case, there is no guaranty that controller of Sec. III will still gives a hierarchical treatment to the control

[1] Because $\operatorname{diag}\{\Delta^*(L^{-1})\}\operatorname{diag}\{\Delta^* E\}$ is always invertible, the use of Δ^* instead of Δ in (6) ensure that $d \mapsto (\lambda, \mu)$ is a bijection whatever are system parameters.

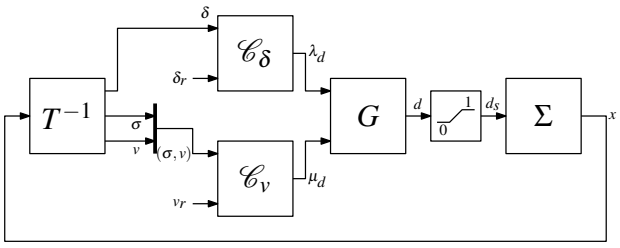

Fig. 2. A first naive solution

objectives. Even more than that, closed-loop might not exhibit appropriate answer at all of the two objectives due to so-called "plant windup" phenomenon which can occur even if static controller is implemented (see [15, Section 1.3]).

V. Solution to Problem 1

Solution exposed in previous section should be regarded as a straightforward adaptation of controller of Sec. III, yet leading as to an *a posteriori* blind treatment of input constraint. Main results of this paper is now exposed and can be conceived as an improvement of solution of Sec. III. Philosophy behind the new approach is to anticipated saturation on d by modifying desired input vector delivered by $\mathscr{C}_\delta$ and $\mathscr{C}_v$ directly *in the new coordinates* (λ, μ). Indeed, the latter being directly related to control goal, hierarchy between objectives can be more easily taken into account when saturating input vector. Thus, this control strategy can be regarded as a post-treatment of desired input complying with ordering of control objectives.

A. First insights for $m = 2$

As a preliminary discussion, let us consider the two converters case ($m = 2$). The (d_1,d_2)-plan is displayed on Fig. 3. Directions of μ and λ are depicted by the grey arrows. Input constraints $[0,1]^2$ are delimited by the red dashed lines.

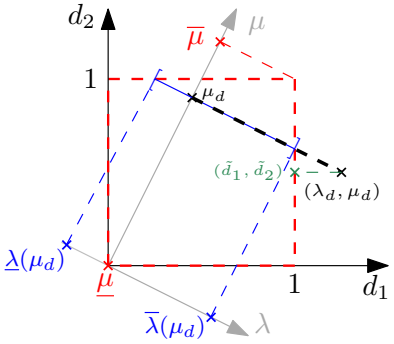

Fig. 3. Saturation principle

Referring to control scheme presented in Sec. III, desired controller output is made of two components: Controller $\mathscr{C}_v$ defined as (9) delivers μ_d to achieve objective (a) whereas $\mathscr{C}_\delta$ defined as (10) provides λ_d and deals with objective (b). Suppose duty cycles corresponding to (μ_d, λ_d) are outside red square as on Fig. 3, i.e. desired control input is unfeasible. Direct saturation of duty cycles as proposed by the naive

solution leads to point $(\tilde{d_1}, \tilde{d_2})$ where $\tilde{d_1} = 1$. Observe that component along μ of this point is no longer μ_d. As a result, saturation impacts input direction related to the objective (a), which might compromises performance and stability related to this foremost goal.

The key point is that this input direction μ could have been preserved by selecting the feasible input in a different way. Indeed, the set of input vector whose μ coordinate is equal to μ_d has a non empty intersection with the red square. This intersection actually corresponds to the continuous blue segment. Hence, there exists feasible input sharing with (λ_d, μ_d) the same coordinate μ. Then, it seems natural to eventually select *among this set* the closest point to (λ_d, μ_d), that is $(\overline{\lambda}(\mu_d), \mu_d)$ in this case. Here, $\underline{\lambda}(\mu_d)$ and $\overline{\lambda}(\mu_d)$ refers bounds of admissible λ coordinate *for a given coordinate* μ_d, see Fig. 3. It is worth mentioning that selected point $(\overline{\lambda}(\mu_d), \mu_d)$ induces larger differences on the λ coordinate than when the naive solution is retained, i.e. coordinate λ corresponding to $(\tilde{d_1}, \tilde{d_2})$ is closer to λ^d than $\overline{\lambda}(\mu_d)$. Yet, this complies with the hierarchy of the control objectives: Objective (a) is pursued as the foremost goal, possibly at the price of sacrificing objective (b).

Clearly, the above strategy is applicable as soon as continuous blue segment is non empty. From Fig. 3, this happens whenever μ_d belongs to $[\underline{\mu}, \overline{\mu}]$ where $\underline{\mu}$ is actually equal to zero. In this interval, there exists feasible control input preserving coordinate μ_d. On the contrary when $\mu_d \notin [\underline{\mu}, \overline{\mu}]$ holds, it seems natural to select duty cycles whose μ coordinate is either $\underline{\mu}$ or $\overline{\mu}$, depending whether $\mu_d > \overline{\mu}$ or $\mu_d < \underline{\mu}$ hold. This, in turn, leads to a unique λ coordinate, since $\overline{\lambda}(\overline{\mu}_d) = \underline{\lambda}(\overline{\mu}_d)$ and $\overline{\lambda}(\underline{\mu}_d) = \underline{\lambda}(\underline{\mu}_d) = 0$ hold.

Let us now relate this strategy with the typology introduced in the introduction. Recall that (i) refers to the case where input constraints limits input direction related to voltage control. This situation has been distinguished from (ii) input reconfiguration can be performed to make input constraints invisible from input direction mentioned above and, in turn, from voltage control itself. Previous discussion can be summarized by identifying (ii) with the case where (λ_d, μ_d) belongs to $\mathbb{R} \times [\underline{\mu}, \overline{\mu}]$ and (i) when this inclusion does not hold. Indeed, for all (λ_d, μ_d) in $\mathbb{R} \times [\underline{\mu}, \overline{\mu}]$, there exists λ such that (λ, μ_d) corresponds to a duty cycles vector in $[0,1]^d$.

B. The general case where m is arbitrary

Previous discussion, conducted in the context where m equal 2, can be generalized for higher dimension. The proposed strategy which aims defining map $(\lambda_d, \mu_d) \mapsto d$, under the constraints that $d = G_{\lambda\to d}\lambda_s + G_{\mu\to d}\mu$ belongs to $[0,1]^m$, reads as follows:

- Disregarding the value of λ_d, μ_s is first chosen as close as possible to the desired value μ_d, and hence possibly equal to μ_d if the latter belongs to some set $[\underline{\mu}, \overline{\mu}]$ to be defined;
- Admissible set $[\underline{\lambda}(\mu_s), \overline{\lambda}(\mu_s)]$ in which λ_s must belong, is computed. Coordinate λ_s is then selected *in this set* as the closest point to λ_d, i.e. λ_s results from saturation of λ_d with respect to $[\underline{\lambda}(\mu), \overline{\lambda}(\mu)]$.

Fig. 4 provides a graphical illustration of this principle.

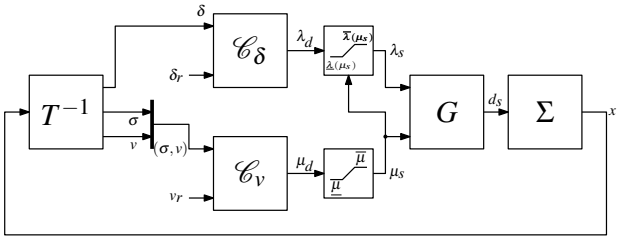

Fig. 4. Control design that solve Problem 1

Remark (A mere unilateral coupling). By saturating input direction in the original coordinate, solution exposed in Sec. IV makes dynamics related (a) dependent of the one corresponding to (b), so that a bilateral coupling is restored, when a mere unilateral coupling was achieved in the unconstrained context of Sec. III. Indeed, back propagation of feasible input set $[0,1]^m$ into (λ, μ) coordinates, one ends up with bounds on μ which are dependent on λ. This implies that desired μ component of input vector (related to (a)) could not be feasible due to desired λ component which is supposed to defined trajectory related to (b). In a way, the proposed strategy settles this conflict by complying with hierarchy of control objectives. By doing so, μ component is made independent of direction λ so that dynamics related to (b) does not impact the one of (a): Coupling still exists (selection of λ depends on μ) but merely in the direction which does not contradicts control hierarchy. ⌟

1) Constraints on μ: The genuine bounds of μ_s is the frontier of the following set

$$\{\mu \in \mathbb{R} : \exists \lambda, G_{\lambda\to d}\lambda + G_{\mu\to d}\mu \in [0,1]^m\}.$$

This set is actually related to the projection of $[0,1]^m$ on the axis corresponding to coordinate μ along the axis corresponding to coordinate λ (λ and μ are not orthogonal in general). Since both $G_{\mu\to d}$ and $[0,1]^m$ belong to nonnegative orthant of $\mathbb{R}^m$ and since every line of $G_{\lambda\to d}$ belongs to either the second or third orthant (depending on the sign of components of $E_\delta L_\delta^{-1}$), $\overline{\mu}$ (resp. $\underline{\mu}$) corresponds to coordinate μ of $\mathbf{1}$ ($\mathbf{0}$). By computing the application $d \mapsto (\lambda, \mu)$, namely G^{-1} which reads

$$G^{-1} = \begin{bmatrix} G_{d\to\lambda} \\ G_{d\to\mu} \end{bmatrix} = \begin{bmatrix} L_\delta E_\delta^{-1} \Gamma_m^\intercal \\ \frac{L_{\text{eq}}}{E_{\text{eq}}} \mathbf{1}_m^\intercal \end{bmatrix} \operatorname{diag}\{L\}^{-1} \operatorname{diag}\{E\},$$

one can compute bounds of μ as

$$\underline{\mu} = G_{d\to\mu}\mathbf{0}_m = 0, \quad \overline{\mu} = G_{d\to\mu}\mathbf{1}_m = \frac{L_{\text{eq}}}{E_{\text{eq}}} \sum_{k\in\mathscr{K}} \frac{E_k}{L_k}.$$

Note that $\operatorname{Im}\{G_{d\to\mu}\} = \operatorname{Ker}\{G_{\lambda\to d}\}$ because $G_{d\to\mu}G_{\lambda\to d} = \mathbf{0}$ so that $G_{d\to\mu}$ is related to the projection on the axis corresponding to coordinate μ along axis corresponding to coordinates λ.

As a conclusion, μ_s derives from μ_d as follows:

$$\mu_s = \begin{cases} \underline{\mu} & \mu_d < \underline{\mu} \\ \mu_d & \mu_d \in [\underline{\mu}, \overline{\mu}] \\ \overline{\mu} & \mu_d > \overline{\mu} \end{cases} \tag{11}$$

2) Constraints on λ: Coordinate λ_s is selected as the closest value to λ_d under the constraints of feasible duty cycles, i.e. such that

$$\begin{aligned} &G_{\mu\to d}\mu_s + G_{\lambda\to d}\lambda \in [0,1]^m \\ &\qquad \Leftrightarrow -G_{\mu\to d}\mu_s \le G_{\lambda\to d}\lambda \le \mathbf{1}_m - G_{\mu\to d}\mu_s \end{aligned} \tag{12}$$

Thus λ_s is computed via the following optimization problem

$$\begin{aligned} \lambda_s \in \quad & \underset{\lambda}{\operatorname{argmin}} ||\lambda - \lambda_d||_2 \\ \text{subject to} \quad & \begin{bmatrix} G_{\lambda\to d} \\ -G_{\lambda\to d} \end{bmatrix} \lambda \le \begin{bmatrix} \mathbf{1}_m - G_{\mu\to d}\mu_s \\ G_{\mu\to d}\mu_s \end{bmatrix} \end{aligned} \tag{13}$$

Remark (About computational aspects). In (13), value of λ_s is only defined implicitly. However, a closed-form solution of this problem can be given in the case of two converters ($m = 2$), by relying on Fig. 3. Indeed, in this case λ is a scalar and inequality constraints of (13) can be reformulated as follows

$$\begin{aligned} &\max\left(-m\frac{E_2}{L_2} + \frac{E_{\text{eq}}}{L_{\text{eq}}}\mu_s, -\frac{E_{\text{eq}}}{L_{\text{eq}}}\mu_s\right) \le \frac{E_\delta}{L_\delta}\lambda \quad \text{and} \\ &\frac{E_\delta}{L_\delta}\lambda \le \min\left(m\frac{E_1}{L_1} - \frac{E_{\text{eq}}}{L_{\text{eq}}}\mu_s, \frac{E_{\text{eq}}}{L_{\text{eq}}}\mu_s\right), \end{aligned}$$

bearing in mind that those inequalities characterized the blue continuous segment depicted on Fig. 3.

Giving an explicit solution of (13) when the number of converters m increase seems rather involved in the general case, though. One way is to use the Fourier-Motzkin elimination algorithm (see [16, Section 2.8]). This algorithm consists in eliminating one by one every input variables from the least important to the most important. Thus we are able to project the projection of the constraint polytopes on the direction of the most important variable and to express constraints of each variables witch depends on all the most important variables. As a result, using this algorithm in our case leads to the expression of bounds of the following constraints

$$\underline{\mu} \le \mu \le \overline{\mu} \quad \text{and} \quad \mathbb{R}^{m-1} \ni \underline{\lambda}(\mu) \le \lambda \le \overline{\lambda}(\mu) \in \mathbb{R}^{m-1},$$

where the least important variables λ saturations depends on the value of μ whereas the opposite is false.

⌟

VI. Simulations

In order to illustrate benefits of a strategy dealing with input constraints in a way that control objective hierarchy is preserved, simulations on the system (2) have been performed on Matlab/Simulink in the case of two converters.

A. Model parameters and reference definition

We consider two parallel converters ($m = 2$) where input voltage are $E_1 = E_2 = 24$ V and inductor values are $L_1 = 0.05$ mH and $L_2 = 2.5$ mH. Capacitor and resistor numerical values are respectively $C = 47$ μF and $R = 5$ Ω. Output voltage has to be regulated to $v_r = 12$ V whereas current repartition has to be regulated to $\delta_r = -3$ A so that when it is possible, converter 2 conveys more current than converter 1 with a difference of 3 A. Recall that $\delta = i_1 - i_2$ and $\sigma = i_1 + i_2$ for $m = 2$. Simulations have been performed for the two following controllers:

- controller (A) depicted in Fig. 2 and corresponding to the naive solution of section IV;
- controller (B) represented by Fig. 4 which is controller of section V.

B. Simulation results

Following guidelines provided by subsection III-B, controller gains are selected as follows:

$$K_v = -\begin{bmatrix} 0.12 & 0.03 \end{bmatrix}, \qquad K_\delta = -2.2 \times 10^8. \tag{14}$$

Fig. 5 (resp. Fig. 7) depicts resulting input and state trajectories with controller (A) (resp .controller (B)). Fig. 6 (resp. Fig. 8) depicts resulting input trajectories in (d_1, d_2)-plan for controller (A) (resp .controller (B)). On top of both Fig. 5 and 7, current trajectories passing through each inductors are depicted. Below, the blue line corresponds to output voltage trajectories whereas the red dash-line depicts the voltage reference v_r. Finally at the bottom, blue and cyan lines represent trajectories of duty cycles d_1 and d_2 and the red line corresponds to the virtual input μ_s. On both Fig. 6 and 8 the magenta curve is the desired input d trajectory, reading $d = G[\lambda_d, \mu_d]^\intercal$ whereas the blue line depicts the real input d_s applied to the system. Finally the red dash-line represents bounds of possible value for d_1 and d_2.

Voltage trajectory v for controller (B) gives better results than for controller (A). Indeed, on Fig. 7 we clearly see that v reaches its reference value faster than on Fig. 5. This is due to the fact that, at the beginning, controller (B) puts $d_1 = 1$ whereas controller (A) leaves d_1 close to 0.5. Indeed, for those first points, only the value of desired d_2 is greater than 1. In order to be as closed to μ_d as possible, d_1 is increased by controller (B) to compensate the fact that d_2 reaches its upper bound. This is depicted in the (d_1, d_2)-plan where, for controller (B) projects magenta curve in such a way that the value of μ_d is preserved, whenever it is possible. Here, projection is actually performed in an oblique way. On the contrary, for controller (A), projection is vertical. In fact, because only d_2 reach the upper bound, this signal is saturated to one and d_1 is not modified.

VII. Conclusion

Further work will focus on considering an unknown resistive load leading to integral action and consequently anti-windup control is also an interesting point to be studied.

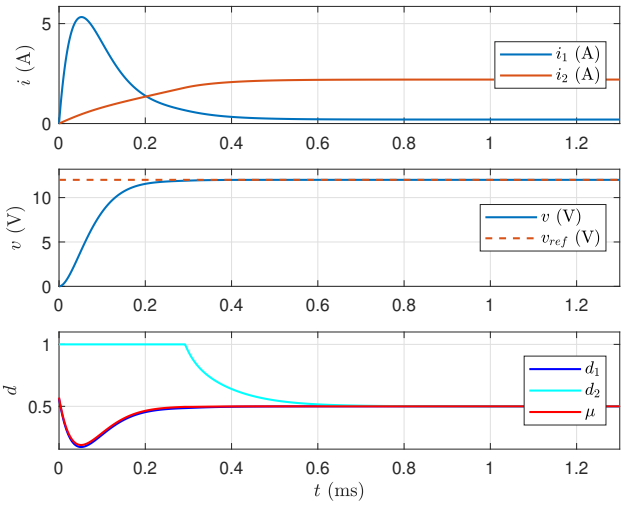

Fig. 5. Chronographs of $v(t)$, $i(t)$, $d(t)$ and $\mu(t)$ for controller (A).

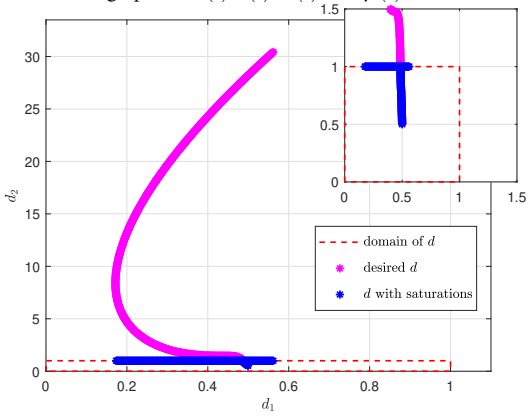

Fig. 6. Results in (d_1, d_2)-plan for controller (A).

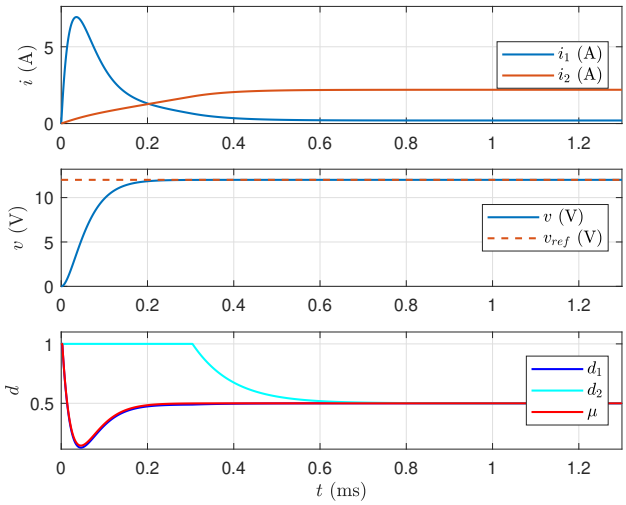

Fig. 7. Chronographs of $v(t)$, $i(t)$, $d(t)$ and $\mu(t)$ for controller (B).

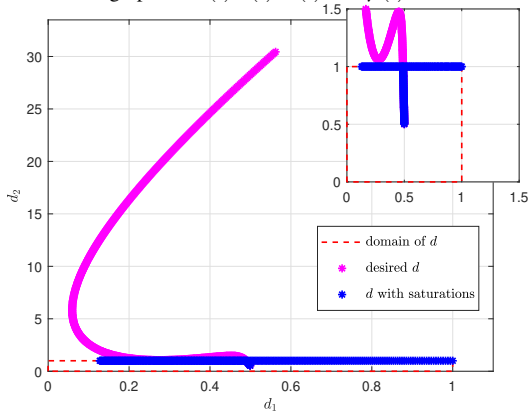

Fig. 8. Results in (d_1, d_2)-plan for controller (B).

References

[1] J. M. Guerrero, J. C. Vásquez, J. Matas, L. G. de Vicuna, and M. Castilla, "Hierarchical control of droop-controlled dc and ac microgrids ; a general approach towards standardization," in *2009 35th Annual Conference of IEEE Industrial Electronics*, Nov 2011, pp. 4305–4310.

[2] V. J. Thottuvelil and G. C. Verghese, "Analysis and control design of paralleled dc/dc converters with current sharing," in *Proceedings of APEC 97 - Applied Power Electronics Conference*, vol. 2, Feb 1997, pp. 638–646 vol.2.

[3] A. Cid-Pastor, R. Giral, J. Calvente, V. I. Utkin, and L. Martinez-Salamero, "Interleaved converters based on sliding-mode control in a ring configuration," *IEEE Transactions on Circuits and Systems I: Regular Papers*, vol. 58, no. 10, pp. 2566–2577, Oct 2011.

[4] J. Sun, Y. Qiu, B. Lu, M. Xu, F. C. Lee, and W. C. Tipton, "Dynamic performance analysis of outer-loop current sharing control for paralleled dc-dc converters," in *Twentieth Annual IEEE Applied Power Electronics Conference and Exposition, 2005. APEC 2005.*, vol. 2, March 2005, pp. 1346–1352 Vol. 2.

[5] Y. Huang and C. K. Tse, "Circuit theoretic classification of parallel connected dc /dc converters," *IEEE Transactions on Circuits and Systems I: Regular Papers*, vol. 54, no. 5, pp. 1099–1108, May 2007.

[6] M. Li, K. T. Chi, H. H. Iu, and X. Ma, "Unified equivalent modeling for stability analysis of parallel-connected dc/dc converters," *IEEE Transactions on Circuits and Systems II: Express Briefs*, vol. 57, no. 11, pp. 898–902, 2010.

[7] S. Luo, Z. Ye, R.-L. Lin, and F. C. Lee, "A classification and evaluation of paralleling methods for power supply modules," in *Power Electronics Specialists Conference, 1999. PESC 99. 30th Annual IEEE*, vol. 2. IEEE, 1999, pp. 901–908.

[8] J.-F. Trégouët and R. Delpoux, "Parallel interconnection of buck converters revisited," *IFAC-PapersOnLine*, vol. 50, no. 1, pp. 15 792 – 15 797, 2017, 20th IFAC World Congress. [Online]. Available: http://www.sciencedirect.com/science/article/pii/S2405896317331324

[9] J. Kreiss, J.-F. Trégouët, R. Delpoux, J.-Y. Gauthier, and X. Lin-Shi, "A geometric point of view on parallel interconnection of buck converters," in *2018 European Control Conference (ECC)*, Limassol, Cyprus, June 2018, pp. 70–75.

[10] H. L. Trentelman, A. A. Stoorvogel, and M. Hautus, *Control theory for linear systems*, 2001st ed., ser. Communications and Control Engineering. Springer-Verlag London, 2012, vol. 1.

[11] W. M. Wonham, *Linear multivariable control: a geometric approach*. Springer-Verlag New York, 2012, vol. 10.

[12] G. Basile and G. Marro, *Controlled and Conditioned Invariants in Linear System Theory/Book and Disk*. Prentice Hall, 1992, vol. 1.

[13] J.-F. Trégouët, R. Delpoux, and J.-Y. Gaulthier, "Optimal secondary control for dc microgrids," in *2016 IEEE 25th International Symposium on Industrial Electronics (ISIE)*, Santa Clara, CA, June 2016, pp. 510–515.

[14] A. Serrani, "Output regulation for over-actuated linear systems via inverse model allocation," in *2012 IEEE 51st IEEE Conference on Decision and Control (CDC)*, Dec 2012, pp. 4871–4876, article avec les graphiques et beaucoup de definitions sur geometrie.

[15] P. Hippe, *Windup in control: its effects and their prevention*. Springer Science & Business Media, 2006.

[16] D. Bertsimas and J. N. Tsitsiklis, *Introduction to linear optimization*, A. Scientific, Ed. Athena Scientific Belmont, MA, 1997, vol. 6.